Reprinted from: THERMAL CONDUCTIVITY, PROCEEDINGS OF THE EIGHTH CONFERENCE (Purdue Univ., West Lafayette, Indiana, Oct 7-10, 1968). Edited by C. Y. Ho and R. E. Taylor. Plenum Press, New York, 1969.

THERMAL CONDUCTIVITY OF AEROSPACE ALLOYS AT CRYOGENIC TEMPERATURES†

J. G. Hust and Robert L. Powell

Cryogenics Division, Institute for Basic Standards

National Bureau of Standards, Boulder, Colorado, 80302

ABSTRACT - Thermal conductivity, electrical resistivity, Lorenz ratio, and thermopower have been determined for several aerospace alloys between 4 and 300 K: titanium A-110 AT, Inconel 718,* Hastelloy X,* and aluminum 7039. These data are presented graphically. By utilizing detailed numerical and theoretical analyses, we have been able to separate the electronic and lattice contributions to the total thermal conductivity. Various scattering mechanisms have also been resolved for both types of conduction. The first three alloys are predominately lattice conductors at low temperatures, with total Lorenz numbers as high as $15 V^2/K^2$ near 20 K.

KEY WORDS - Aluminum 7039, cryogenic temperatures, electrical resistivity, Hastelloy-X, Inconel 718, Lorenz ratio, nickel alloy, thermal conductivity, thermopower, titanium alloy, titanium A-110 AT.

I. INTRODUCTION

Design and development engineers in the aerospace industry continue to have urgent need for thermal and mechanical property data for new materials. For most materials, especially uncommon alloys, measured values of thermal conductivity are not available and predictions cannot yet be made with adequate confidence. To help satisfy the immediate need for such data we are making thermal conductivity measurements on several alloys of direct interest to NASA.

† This work was carried out at the National Bureau of Standards under the sponsorship of the National Aeronautics and Space Administration, Space Nuclear Propulsion Office, Cleveland. Not subject to copyright.

* The use in this paper of trade names of specific products is essential to a proper understanding of the work presented. Their use in no way implies any approval, endorsement, or recommendation by NBS. See item [6] in "References" for a list of trade name designations.

Because accurate low temperature measurements of thermal conductivity are expensive and time consuming, no standards laboratory can hope to measure all technically important materials over a wide temperature range. For this reason the work at NBS includes the measurement and characterization of standard reference materials which will encourage and facilitate measurements at other laboratories. We are also measuring the thermopower and electrical resistivity of each specimen to enhance our ability to predict thermal conductivity of unmeasured materials by using the more readily obtained electrical resistivity data and Lorenz ratio analysis. This program is directed toward the acquisition of thermal conductivity data with an accuracy of about 1% or better at temperatures from 4 to 300 K.

Data are reported here for titanium A-110 AT, aluminum 7039, Inconel 718, and Hastelloy X. Preliminary data for titanium A-110 AT and aluminum 7039 were presented [1][1] last year at the 7th Thermal Conductivity Conference. The data presented here are final values based upon more sophisticated data analysis and more accurate thermocouple calibration tables.

Measurements have also been completed for a specimen of Armco iron, PO-3 graphite and reactor grade beryllium. These data however are still in preliminary form and will be presented in a later publication.

II. METHOD OF MEASUREMENT AND APPARATUS

The apparatus used is based on the axial one-dimensional heat flow method. The specimen is a cylindrical rod with a heater at one end and temperature controlled heat sink at the other. The heat sink is controlled to any temperature from 4 to 300 K by means of several cryogenic baths and an automatic electronic temperature controller. The sample assembly is surrounded by a cylindrical temperature controlled shield to reduce heat losses by conduction and radiation. To further reduce losses by radiation the space between the shield and the specimen is filled with high-density glass fibers. The entire sample-shield assembly is enclosed in a container and evacuated to less than 10^{-5} torr (1.3×10^{-3} N/m^2). A detailed description of this apparatus was presented at the 7th Thermal Conductivity Conference [1].

III. RESULTS

Table I lists specimen diameter, composition, and fabrication condition for the materials measured. Also included in Table I are hardness and grain size of each specimen.

[1] Numbers in brackets designate references listed at the end of this paper.

The thermal conductivities of the measured specimens are presented in figure 1. The curves were calculated from equations fitted to the experimental data. The equations represent the data to approximately their inherent random scatter; thus the fit does not contribute significant systematic error nor does it result in oscillations due to overfitting. The electrical resistivity data are presented in figures 2 and 3. Note that the values for titanium A-110 AT, Hastelloy X and Inconel 718 (fig. 2) are large and change by only a few percent over the entire range because of the high percentage of alloying. The minima at low temperatures ($\sim$ 20 K) for these three specimens is evidence of magnetic ordering, possibly the Kondo effect [2]. The electrical resistivity of aluminum does not exhibit a minimum at low temperatures and changes by about a factor of three from 4 to 300 K. The Lorenz ratios of these specimens are given in figures 4 and 5. For the specimens of titanium A-110 AT, Hastelloy X and Inconel 718 it is obvious from the high Lorenz ratios at low temperature that the lattice contribution to the total conductivity is about six times greater than the electron contribution. Such high lattice contributions are often alluded to in the literature for alloys but not often confirmed experimentally. Similar curves are expected for other low temperature structural alloys. The thermopowers of these alloys with respect to "normal" silver (Ag - 0.37 atomic % Au) are presented in figure 6.

Table I

Material, Diameter	Condition (Structure)	Rockwell Hardness	Av. Grain Size (mm)	Composition Weight % (values listed if > 0.1%)
Ti-A110AT 1.13 cm	Annealed (HCP)	C-35	0.015	Ti-bal, Al-5.5, Sn-2.5, Fe-0.2, C, N, H.
Al 7039 0.367 cm	T 61 (FCC)	B-75	0.005 (10:1 elongation with sample length)	Al-bal, Zn-3.6, Mg-2.55, Mn-0.23, Cr-0.20, Fe, Cu, Si, Ti, Be
Inconel 718 1.13 cm	Age-hardened (BCC + FCC ppt)	C-39	0.06	Ni-54.57, Cr-18.06, Fe-17.08, Nb + Ta-5.12, Mo-3.18, Ti-0.85, Al 0.44, Mn-0.29, Si-0.24, Cu, C, S.
Hastelloy X 1.13 cm	Annealed (BCC + FCC ppt)	B-88	0.08	Ni-bal, Cr-21.06, Fe-17.58, Mo-9.15, Co-1.45, W-0.65, Mn-0.53, Si-0.43, C-0.12, P, S.

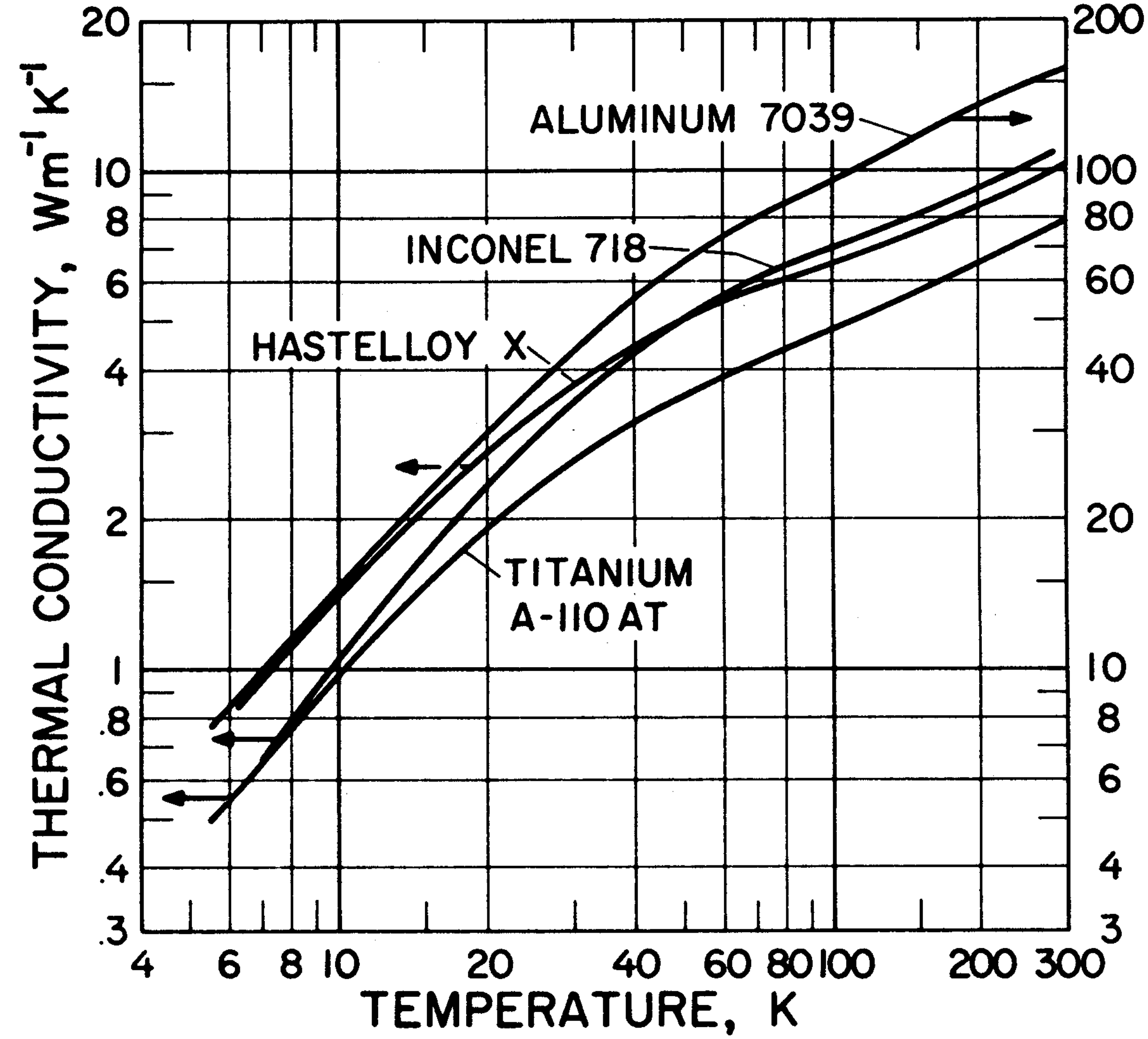

Figure 1. Thermal Conductivity of titanium A-110 AT, aluminum 7039, Inconel 718 and Hastelloy X.

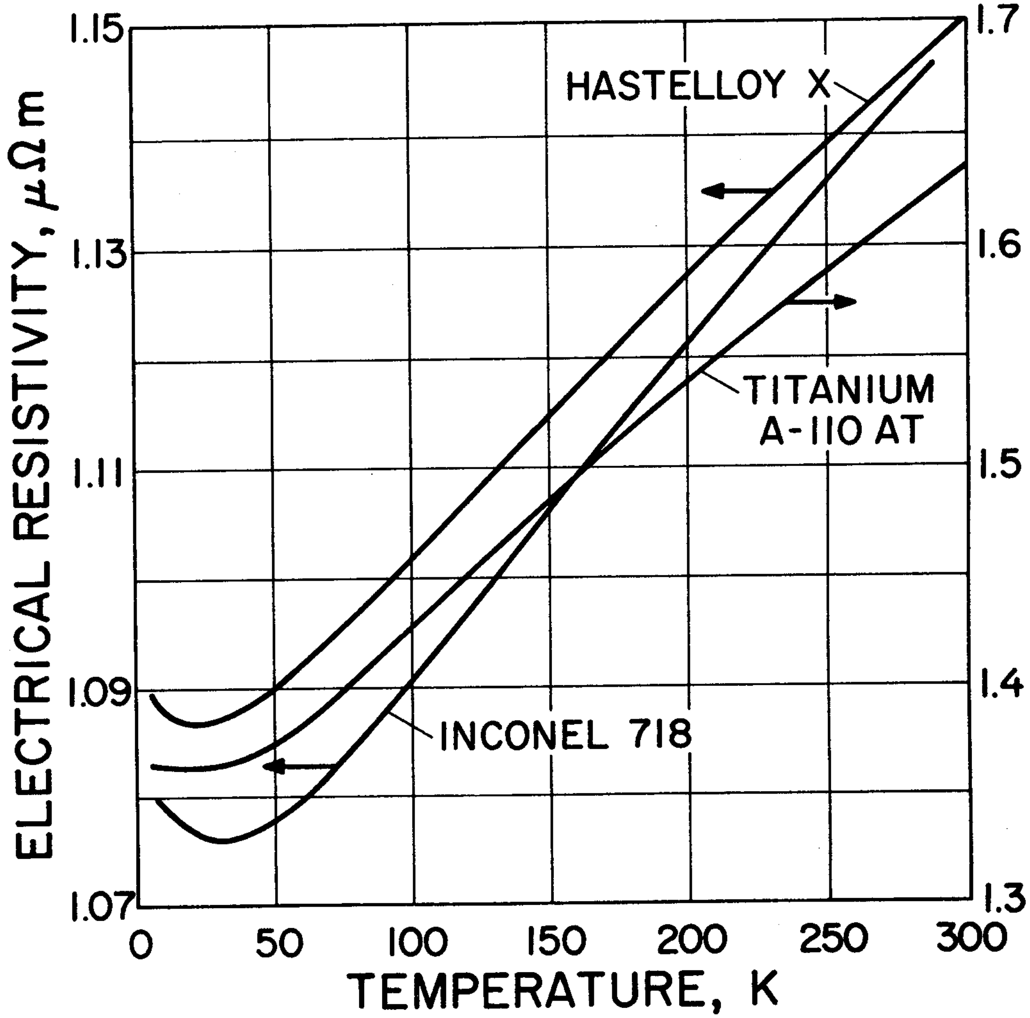

Figure 2. Electrical Resistivity of titanium A-110 AT, Inconel 718, and Hastelloy X.

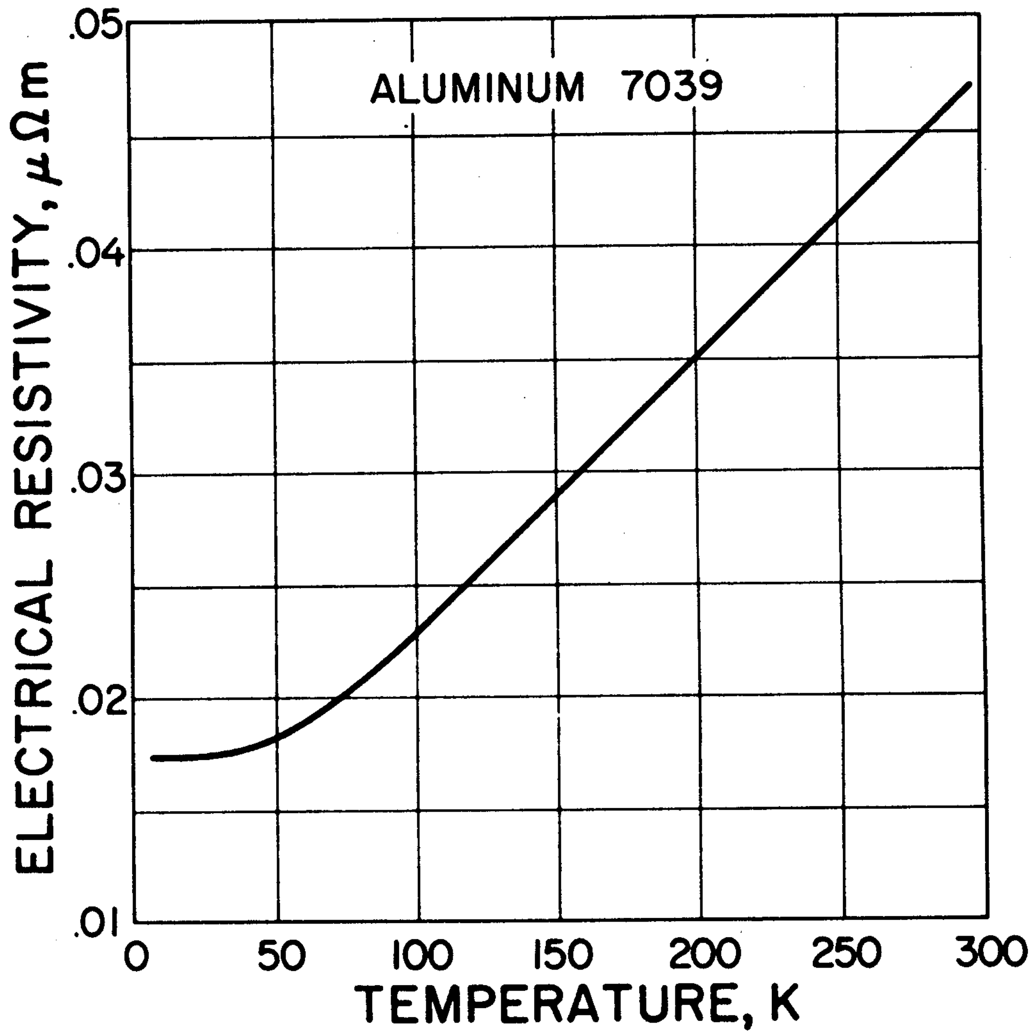

Figure 3. Electrical Resistivity of aluminum 7039.

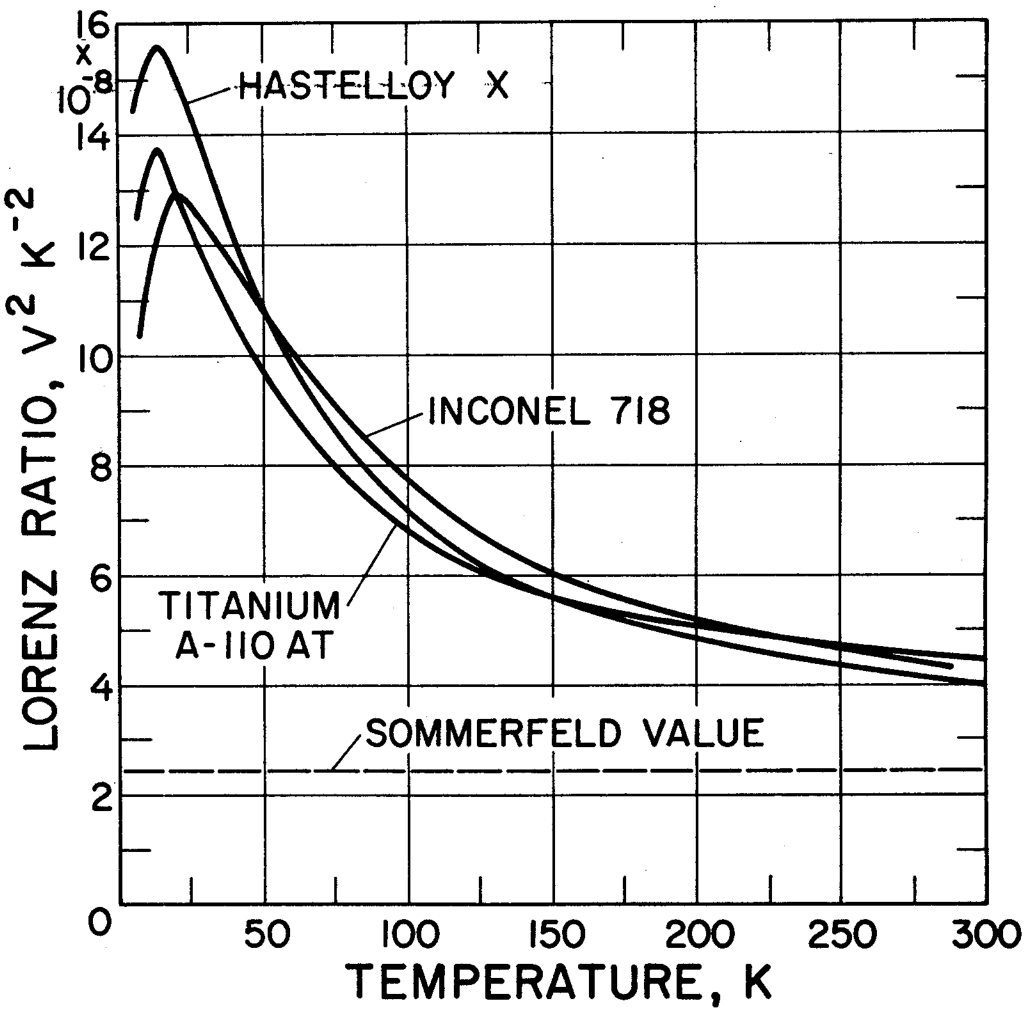

Figure 4. Lorenz number of titanium A-110 AT, Inconel 718, and Hastelloy X.

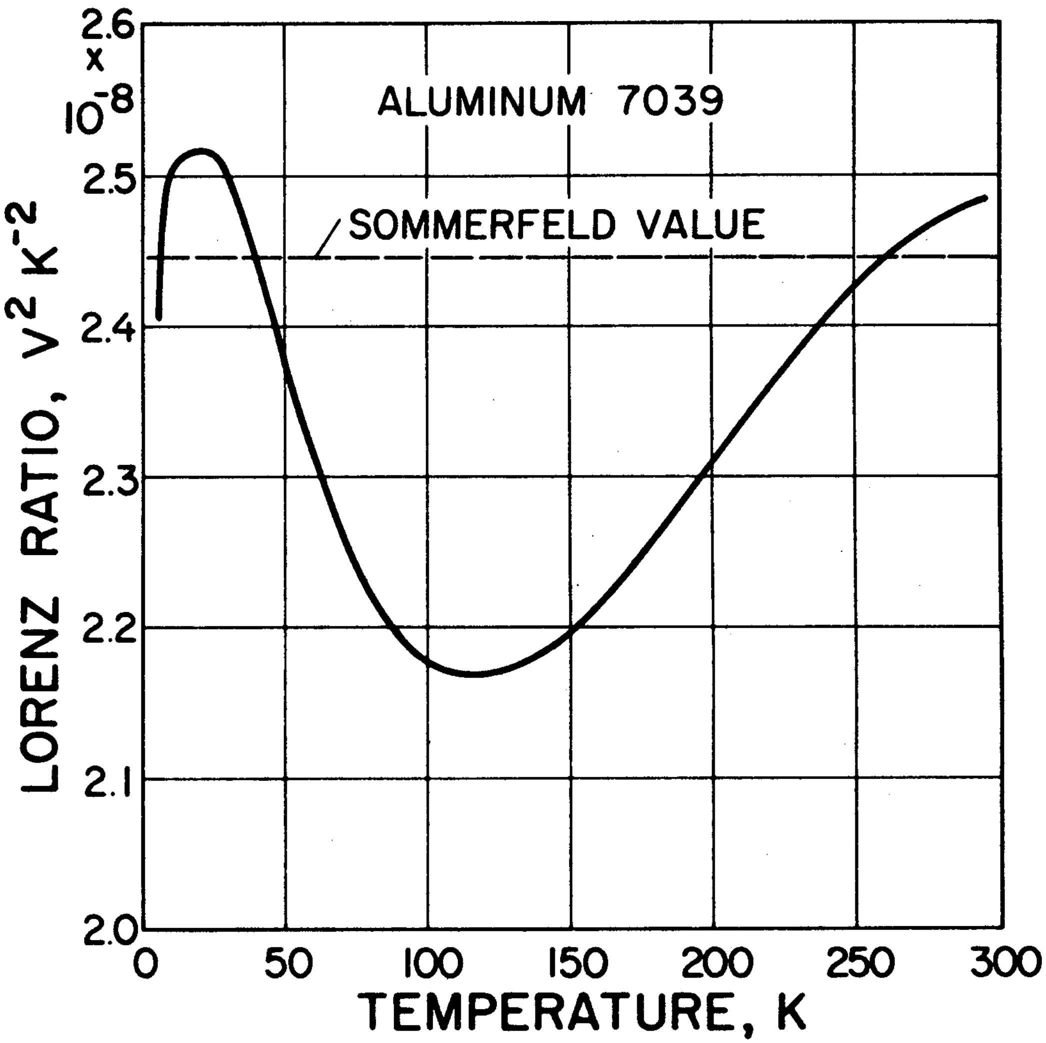

Figure 5. Lorenz number of aluminum 7039.

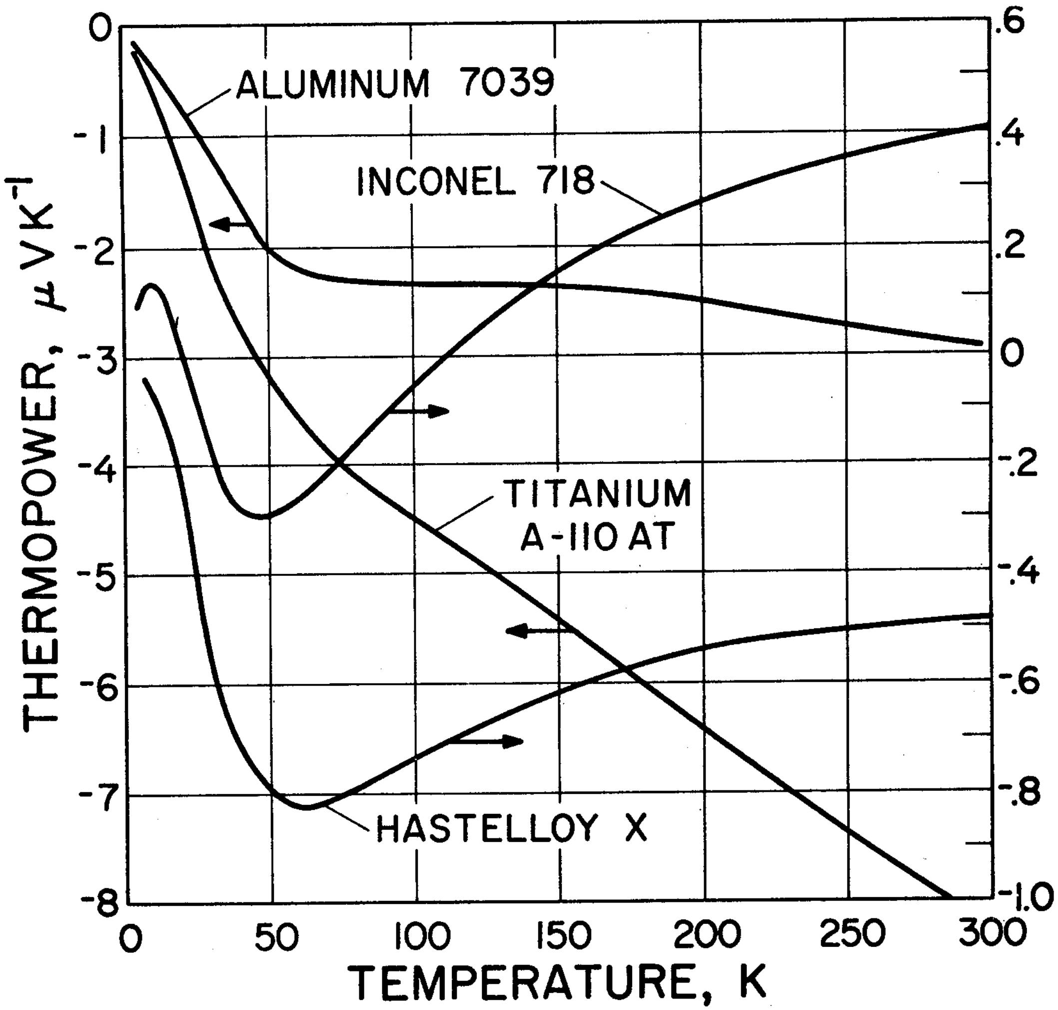

Figure 6. Thermopower of titanium A-110 AT, aluminum 7039, Inconel 718, and Hastelloy X.

IV. DISCUSSION

Preliminary component analyses of the thermal conductivity data have been accomplished to determine the scattering mechanisms affecting the lattice component of the conductivity. The separation of components has been carried out as follows:

We assume additivity of electronic (λ_e) and lattice (λ_g) thermal conductivities, i.e.,

$$\lambda = \lambda_e + \lambda_g \ . \tag{1}$$

The reciprocal of the electronic conductivity, the thermal resistivity, W_e, is separated into impurity (W_o), intrinsic (W_i), and interaction (W_{io}) components:

$$\lambda_e^{-1} \equiv W_e = W_o + W_i + W_{io} \equiv W_o + W_I. \tag{2}$$

The electrical resistivity can be similarly separated:

$$\rho = \rho_o + \rho_i + \rho_{io} = \rho_o + \rho_I \ . \tag{2a}$$

The impurity component, W_o, is computed from the Wiedemann-Franz law

$$W_o = \frac{\rho_o}{L_s T}, \tag{3}$$

where L_s = Sommerfeld value of Lorenz ratio and ρ_o is the residual electrical resistivity.

The sum of intrinsic and interaction terms, $W_I \equiv W_i + W_{io}$, is computed from

$$W_I = \frac{\rho_I}{L_i T}, \tag{4}$$

where L_i is the intrinsic Lorenz ratio and ρ_I is the sum of intrinsic plus interaction electrical resistivities.

Equation (4) is obtained as follows:

The interaction terms W_{io} and ρ_{io} are assumed to be of the form

$$W_{io} = \frac{\alpha W_i W_o}{\beta W_o + \gamma W_i} \tag{5}$$

$$\rho_{io} = \frac{\alpha \rho_i \rho_o}{\beta \rho_o + \gamma \rho_i} \tag{6}$$

where α, β, and γ are constants near unity. The intrinsic Lorenz ratio is defined by

$$W_i = \frac{\rho_i}{L_i T} \ . \tag{7}$$

The value of L_i, as obtained from other measurements and theory, approaches L_s at high temperature and falls to zero quadratically at very low temperature.

The intrinsic Lorenz ratio is obtained from data reported by White and Woods [3] for copper, sodium, and several transition elements. These data ($L_i = \rho_i / W_i T$) were plotted versus T/θ_D, where θ_D is the Debye temperature. An average curve weighted heavily toward copper was drawn and used for L_i values in this work. There is a relatively large uncertainty here because of the spread in the curves for different materials, however, since W_i is small compared to W_o for the materials investigated, the overall error in W_o is small. Values of L_i versus T/θ_D are given in table II.

Table II

L_i V^2/K^2	T/θ_D	L_i V^2/K^2	T/θ_D
$0 \quad \times 10^{-8}$	0	2.02×10^{-8}	.45
.32	.05	2.10	.50
.80	.10	2.23	.60
1.12	.15	2.32	.70
1.35	.20	2.37	.80
1.53	.25	2.40	.90
1.69	.30	2.42	1.00
1.81	.35	2.43	1.50
1.92	.40	2.44	2.00

Combining equation (3), (5), (6) and (7) we obtain

$$W_I = W_i + W_{io} = \frac{\rho_i}{L_i T} + \frac{\alpha \rho_i \rho_o}{T(\beta \rho_o L_i + \gamma \rho_i L_s)} \tag{8}$$

Since $\rho_i << \rho_o$, $W_I << W_o$ at low temperatures, and L_i approaches L_s at high temperatures, we can obtain a further simplification with little loss of accuracy:

$$W_e = W_o + W_I \approx W_o + \frac{1}{L_i T}\left[\rho_i + \frac{\alpha \rho_i \rho_o}{\beta \rho_i + \gamma \rho_o}\right] = W_o + \frac{\rho_I}{L_i T} \, . \tag{9}$$

We thus obtain the electronic thermal conductivity component

$$\lambda_e = W_e^{-1} = \left(\frac{\rho_o}{L_s T} + \frac{\rho - \rho_o}{L_i T}\right)^{-1} \, . \tag{10}$$

We then obtain the lattice thermal conductivity component from (1) and (10):

$$\lambda_g = \lambda - \left(\frac{\rho_o}{L_s T} + \frac{\rho - \rho_o}{L_i T}\right)^{-1} \, . \tag{11}$$

The analysis of lattice conductivities is not yet completed; however, some preliminary remarks seem appropriate. At low temperatures λ_g for these specimens as calculated from equation (11) varies as T^n where n in all cases is between 1 and 2. The value of n = 2 would be expected if the phonons were scattered primarily by electrons and dislocations. However an exponent nearer unity, is observed. This suggests the possibility of considerable scattering by planar defects such as stacking faults or laminar precipitates at grain boundaries. Pippard [4] derived the temperature dependence of the lattice conductivity for the case of phonons with wavelengths larger than the mean-free-path of interacting electrons. This scattering mechanism results in $\lambda_g \propto T$ also. The value of n for the Inconel 718 specimen is somewhat larger than for the other specimens, thus indicating the presence of significant dislocation scattering. At high temperatures the λ_g versus T curves decrease in slope indicating the presence of significant point imperfection scattering and possibly umklapp scattering. At this time it is difficult to be sure of which scattering mechanisms are present, especially at the lower temperatures. However it is likely that the mechanism described by Pippard [4] is in part responsible for the observed behavior of λ_g. Similar behavior was observed in silver-antimony alloys below 4K by Zimmerman [5]. Further metallurgical investigations on these specimens may lead to a better understanding of the mechanisms present. The details of this work will be published in the near future.

V. REFERENCES

[1] Hust, J. G., Weitzel, D. H., Powell, Robert L., "Thermal Conductivity of Aerospace Alloys at Cryogenic Temperatures," Proc. of the Seventh Thermal Conductivity Conference, NBS, Gaithersburg, Maryland, Nov. 13-16, 1967, pp. 271-8.

[2] Kondo, J., Resistance Minimum in Dilute Magnetic Alloys, Prog. Theoret, Phys. 32, 37-49 (1964).

[3] White, G. K., and Woods, S. B., Electrical and Thermal Resistivity of the Transition Elements at Low Temperatures, Phil. Trans. Roy. Soc. A251, 273-302 (1959).

[4] Pippard, A. B., Ultrasonic Attenuation in Metals, Phil. Mag. 46, 1104-14 (1955).

[5] Zimmerman, J. E., Low-Temperature Lattice Heat Conduction in High-Resistivity Alloys, J. Phys. Chem. Solids 11, 299-302 (1959).

[6] Armco iron is the registered trade name for a commercially pure iron produced by Armco Steel Corporation.

Hastelloy is the registered trade name for a nickel-chromium-iron alloy produced by Union Carbide Corp., Stellite Division.

Inconel is the registered trade name for a nickel-chromium-iron alloy produced by International Nickel Corporation.

PO-3 is the registered trade name for a graphite produced by Pure Carbon Company.